Materials Today Communications 26 (2021) 101942

Contents lists available at ScienceDirect

Materials Today Communications

journal homepage: www.elsevier.com/locate/mtcomm

Novel natural spider silk embedded electrospun nanofiber mats for wound healing

Kerim Emre Öksüz [a,*], Nese Kurt Özkaya [b], Zeynep Deniz Şahin İnan [c], Ali Özer [a]

[a] Sivas Cumhuriyet University, Department of Metallurgical and Materials Engineering, Sivas, 58140, Turkey
[b] Sivas Cumhuriyet University, Department of Plastic, Reconstructive and Aesthetic Surgery, Faculty of Medicine, Sivas, 58140, Turkey
[c] Sivas Cumhuriyet University, Department of Histology-Embryology, Faculty of Medicine, Sivas, 58140, Turkey

ARTICLE INFO

Keywords:
Biomaterials
Electrospinning
Silk fibers
Surgical wounds
Wound dressing

ABSTRACT

In recent years, electrospun nanofiber mats based on biopolymers have been extensively investigated for tissue and biomedical engineering, mainly because of remarkable morphological similarity with the natural extracellular matrix. The current study focuses on the preparation of novel natural spider silk (SS) embedded Poly(vinyl alcohol)(PVA)/Sodium alginate (NaAlg) wound dressings with desirable properties for a wound dressing application. The nanofibers' surface morphology and structure were observed by a field emission scanning electron microscope (FE-SEM). *In-vivo* evaluation of PVA/NaAlg based electrospun nanofiber mats as a wound dressing material and their comparison to commercially available wound dressings was carried out by *in-vivo* tests on rabbit models. Some morphometric parameters such as counting cells, blood vessels, endothelial cells, determination of the area of the wound closure, wound healing performance, speed of wound healing and collagen thickness were investigated using OM and FE-SEM post-processing. Furthermore, *in-vitro* biocompatibility and cellular behavior such as adhesion and proliferation of mouse fibroblast cells (L929) were studied by XTT assay on developed nanofiber mats. The results of this experimental study indicated that the natural spider silk embedded electrospun nanofiber mat (PVA/NaAlg/SS) accelerated the rate of wound healing compared to other groups by improving the collagen formation rate, proliferative cell activity as well as decreasing the inflammatory cell amount. Furthermore, the results of the *in-vivo* and *in-vitro* experiments suggest that novel PVA/NaAlg/SS nanofiber mats might be a fascinating bioactive wound dressing for clinical applications.

1. Introduction

Materials produced by electrospinning technology present extraordinary surface area, fine-sized pores, and three-dimensional (conformal) organization, making them ideal candidates for next-generation wound dressing applications. These superior features are very favorable for the absorption of body fluids and prevent the penetration of microbial colonization and thus provide excellent conditions for wound healing [1,2]. The tissue and materials engineering sciences are aimed to study more modern, practical, and comfortable wound dressings that support the healing of tissue wounds as soon as possible and the accelerated formation of new collagen in living tissue.

In recent years, there has been growing attention to fabricating electrospun nanofiber mats based on natural and synthetic biopolymers via a commonly used technique of electrospinning for wound dressing applications. Electrospun materials possess extended properties like high mechanical strength, high specific surface area, high porosity, large length-to-diameter ratio, etc., which make them novel to be used in various applications. Electrospun nanofibers can be manipulated by coordinating, stacking, or folding to make variants of the material such as electrospun membranes, electrospun mats, electrospun composites, etc. Additives in these electrospun variants are usually applied during the electrospinning procedure, thereby enabling the modification of different properties according to the desired applications [3].

Compared to synthetic polymers, natural polymers have been used more due to their better biocompatibility, lower immunogenicity, and better clinical features. Besides, natural polymers are less toxic, biodegradable, and do not contain any synthetic chemical as synthetic polymers and derivatives include [4,5]. Among them, silk fibroin (SF), extracted from living creatures (e.g., Bombyx mori silkworm cocoons, spiders, scorpions), have recently gained attention because of its unique biological behavior, biocompatibility, biodegradability, high water, and

* Corresponding author.
E-mail address: emre.oksuz@cumhuriyet.edu.tr (K.E. Öksüz).

https://doi.org/10.1016/j.mtcomm.2020.101942
Received 14 May 2020; Received in revised form 6 November 2020; Accepted 28 November 2020
Available online 2 December 2020

oxygen uptake, low immunogenicity, and sturdy mechanical properties [6–8].

The combination of the natural polymers and the spider silks offers excellent opportunities in engineering innovation, functional materials for a wide range of biomedical applications [9]. We have recently investigated some biomedical applications of natural spider silk embedded PVA/NaAlg nanofiber mats; here, we summarize our study utilizing spider silk derived from the natural process as a wound dressing. We believe these are very limited reports which need to study by further investigations on the use of natural spider silk grafted biopolymers for biomedical applications as wound dressing [10–12].

2. Materials and methods

2.1. Materials

The Sodium Alginate polymer and Poly (vinyl) Alcohol polymer were purchased from Sigma Aldrich (USA). Medical, commercial wound dressing (Aquacel®-Ag) was purchased from the ConvaTec Group PLC Company (USA). The cotton gauze was bought from the local biomedical company (Turkey). All other chemicals used in this study were of analytical grade and were used without further purification and were purchased from *the Merck, Sigma Aldrich and Thermo Fisher Scientific* Company (USA).

2.2. Preparation of the electrospun nanofiber mats

The NaAlg solution with a concentration of 1% (w/v) and the PVA solution with a concentration of 9% (w/v) were blended in the volume ratio of 2/1 PVA/NaAlg. The PVA/NaAlg blend solution was placed in a 5-mL plastic syringe equipped with a flat-end metal needle with an inner diameter of 0.7 mm. The stainless steel needle of the syringe was connected to the positive electrode by a copper wire. A flat piece of aluminum foil, connected to the negative electrode, was used to collect the polymeric nanofibers mat. A direct-current power supply supplied a 14 kV voltage, and the feed rate of the polymer solution was adjusted to a constant rate of 0.3 mL h^{-1}. A ground collection plate of aluminum foil was located at a fixed distance of 100 mm from the needle tip. At the end of the electrospinning process, the nanofibers deposited in the collector were carefully stripped and dried at room temperature under a vacuum.

The giant house spiders (Tegenaria gigantea) belong to the family of Agelenidae were picked from their natural environments. The spiders used for this study were kept in a clean glass aquarium in an appropriate and controlled place under enough light and food. Spider silks were kept under eye control for 6 months and the spider silk was picked carefully from spiders without any dust and impurity, weekly. After this procedure, the spiders were released back to nature again. The picked spider silks were transferred to the UV sterilization unit. Spider silks were used right after UV sterilization and kept in sealed and sterile Petri dishes. The collected and UV sterilized spider silk was weighed with a precision balance with a sensitivity of 10^{-5} g. 20 ± 4 mg of silk was weighed and laid on a 2 × 2 cm square PVA/NaAlg nanofiber mats. Then, it was pressed under 100 kPa pressure to ensure the embedding of silk on mats. The mats' total weight was founded approximately 500 ± 18 mg (5 wt. % of mats).

2.3. Characterization of the electrospun nanofiber mats

The average porosity (%), degree of swelling (%) and water vapor transmission rate (g/m^2.24 h) of the sample groups were determined according to the procedure as described in detail elsewhere [8,13]. Field emission scanning electron microscopy (FE-SEM, Tescan® Mira3 XMU, Brno, Czechia) was used to measure fiber diameters and the surface morphology of PVA/NaAlg, PVA/NaAlg/SS nanofiber mats and natural spider silk.

2.4. In-vitro biocompatibility studies

The *in-vitro* cytotoxicity of the cotton gauze, Aquacel®-Ag, PVA/NaAlg, and PVA/NaAlg/SS nanofiber mats was assessed according to ISO 10993-5 standard test method. The antiproliferative activities of the samples were measured via XTT reagent (2, 3-bis-(2-methoxy-4-nitro-5-sulfophenyl)-2H-tetrazolium-5-carboxanilide) colorimetric assay. The samples were cut out with a punch (5-mm in diameter) and they were sterilized under UV light for 1 h on each side. After incubation, the compounds were dissolved in cell culture grade dimethyl sulfoxide (DMSO concentration did not exceed 0.1 %) and diluted in DMEM before treatment. The cells were treated with 10 μM constant concentrations of compounds or vehicle (0.1 % DMSO) for 24 h. Afterward, the culture medium was aspirated and replaced by 100 μL of fresh colorless DMEM. For the determination of living cells, 50 μL XTT labeling mixture was added to each well, and then the plates were maintained in a wet atmosphere containing 5 vol% CO_2 and 37 °C in for 4 h. Consequently, the viability of cultured cells was obtained by colorimetric XTT assay using an ELISA microplate reader (Thermo Scientific™, Germany) based on optical density (OD) detection at 450 nm. All experiments were performed in triplicate and the cell viability was expressed in percentage related to control (100 % of viability). In parallel, cell attachment to the samples was evaluated at 24 h. Cells were allowed to grow for 24 h in complete medium at 37 °C and 5% CO_2. After 24 h, the culture medium was removed and cells were fixed with 2.5 % glutaraldehyde fixative for 2 h at 4 °C. Then the samples were washed PBS and dehydrated in graded ethanol series. The samples were fixed on aluminum stubs and pre-coated with gold/palladium thin film for 5 min. under argon atmosphere and then the attached cells on samples were visualized using a FE-SEM [14–16].

2.5. In-vivo studies

Approval was obtained from the Animal Research Ethics Committee of our Medicine Faculty Research Hospital (dated 26.02.2019 and 65202830−050.04.04-264 numbered). Each five months old, with an average weight of 2.7–3.0 kg, of which eight male New Zealand white rabbits were used. Rabbits were fed and protected in appropriate conditions. Each rabbit was injected intramuscularly 5 mg/kg Xylazine - 35 mg/kg ketamine HCl and subcutaneously analgesic drug (4 mg/kg) Carprofen. After anesthetized was inflicted and prepared, four wounds were created on the backs of each animal approximately equidistant from each other by removing skin up to the panniculus carnosus at the floor's base from the back of the animals and hemostasis was achieved with gauze pressure to the wound created. Thus, each rabbit included 4 study groups: Control, Aquacel®, PVA/NaAlg, and PVA/NaAlg/SS groups. Eight animals in total were used. All the surgical procedures were performed by the same surgeon (N.K.O), and by performing using aseptic technique, and powderless gloves were used in all surgeries. The wound healing was configured as follows:

Control (C) group; In the control group, the wounded areas were not treated with any dressing. Wound healing was followed only macroscopically.

Aquacel®-Ag group; In the lower-left quadrant, the wound was spread with a sterilized layer of Aquacel®-Ag.

PVA/NaAlg group; The wound in the right upper quadrant was spread (replenished) every three days and was treated with a thin layer of PVA/NaAlg nanofiber mat sterilized under ultraviolet light for one night.

PVA/NaAlg/SS group; The wound in the left upper quadrant was spread in every three days with a thin layer of natural spider silk protein sterilized under ultraviolet light for one night.

2.6. Tissue preparation & histological studies

The specimens were fixed in 10 wt. % buffered neutral formalin for

24−48 h, dehydrated through ascending ethanol is cleared in xylene, embedded in paraffin and were taken from the paraffin blocks (4−5 μm). The sections were stained with hematoxylin-eosin (H&E) to assess the wound region's healing area, the rate of inflammation, the amount of collagen fiber in the connective tissue, and epithelization [17]. Immunohistochemically staining was performed in the sections to determine the vascular structure at the wound site. For immunohistochemistry (IHC) tissue sections on microscope slides were dewaxed and rehydrated, treated with 3 w.t % H_2O_2 and sections were microwaved in EDTA buffer. Normal blocking serum was placed on all slides and treated with goat anti-rabbit biotinylated secondary antibodies and avidin-biotin-horseradish peroxidase complex reagent. Then treated with 3-Amino-9-Ethylcarbazole twice for 5 min. and counterstained with hematoxylin. The primary antibody included vascular endothelial growth factor (VEGF) *Ab-1* (diluted; ready to use). The wound site was evaluated using a light microscope (Olympus BX51, Tokyo, Japan) and staining intensity was scored by two histopathologists using a semi-quantitative scale: 0, none; 1, weak; 2, lightweight; 3, dense; 4, very intense [18–22].

2.7. Tissue preparation for FE-SEM

The tissue sections of 2−3 μm from paraffin-blocked tissues were taken on 18 × 18 coverslip. Sections taken on coverslips were stored at 60 °C in a drying oven for one night for physical deparaffinization. Then, for chemical deparaffinization, it was kept in xylol for one day. FE-SEM examined the surface morphology and quantity of collagen of the paraffin-blocked tissues. The samples were fixed on aluminum stubs and pre-coated with gold/palladium thin film for 5 min. under argon atmosphere using a Quorum RS150 (Birmingham, UK) sputter coater. The FE-SEM samples were examined at an accelerating voltage of 10 kV.

2.8. Statistical & data analysis

The mean and standard deviation values were calculated by measuring at least 20 nanofibers' diameters based on the FE-SEM post-process images to measure fiber diameters of PVA/NaAlg nanofiber mats and natural spider silk. The quantitative data in cell assays were analyzed with Sigma Plot ver. 12.0 (USA), and were presented as mean ± standard deviation. A one-way ANOVA with post hoc Dunn's test or Mann-Whitney test was evaluated with significant differences between samples. P-value <0.05 was considered statistically significant.

Macroscopic appearance and changes of the wounds, whether there was a secretion or not, the size were evaluated on days 0, 4, 7, 12, 15, 18, 21. To identify the wound diameters (mm) before histological measurements, the initial circle diameters were estimated to 20 mm for all of the wound areas. The first approximation was adjusted to 20 ± 2 mm as a quantitative evaluation of measuring points for standard deviation, averaged from five different points measuring by a caliper. By healing days, the average diameters were measured to evaluate the decrease in diameter and plotted accordingly day by day until no wound was seen at the end of day 21. The thickness of collagen in all groups was measured by the linear intercept method on the obtained FE-SEM photos in texture analyses of collagens.

3. Results and discussion

3.1. Characterization of electrospun nanofiber mats

Table 1shows the porosity (%), degree of swelling (%) and water vapor transmission rate (g/m^2.24 h) of the samples. As indicated, as the spider silk was embedded in PVA/NaAlg nanofiber mat, the porosity increases due to increased lighter material on the mat. The degree of swelling is about twice the actual weight and increases by spider silk on PVA/NaAlg nanofiber mats. Since the spider silk and PVA/NaAlg nanofiber (only PVA/NaAlg were mixed together and cross-linked with 2.5 % (w/v) glutaraldehyde solution after electrospinning) mats were not excess cross-linked, the swelling degree increases due to water absorption of polymers. The inner porosity of both PVA/NaAlg and PVA/NaAlg/SS is higher than cotton gauze, the mentioned diameter of fibers decreases but in more rigid laminate forms.

Table 1
Porosity, degree of swelling and water vapor transmission rate properties of the samples.

Samples	Porosity (%)	Degree of swelling (%)	WVTR (g/m^2.24 h; STD: 10%)
Cotton gauze	94 ± 3.12	75 ± 4	1304
Aquacel®- Ag	95 ± 3.74	130 ± 8.5	1152
PVA/NaAlg	96.5 ± 4.42	102 ± 14	986
PVA/NaAlg/SS	98 ± 3.22	105 ± 9	924

Water vapor transmission rate (WVTR) is a measure of long term water vapor formation and transmission rate of vapor away from the surface of studying materials in 24 h. As found out, the cotton gauze has larger pores and larger fibers, the transmission rate is the highest followed by Aquacel®-Ag. PVA/NaAlg nanofiber mats have an approximate diameter of 150 nm while PVA/NaAlg/SS nanofiber mats have a mixed diameter of around 100−500 nm with a spread variation. Since the finer diameter of PVA/NaAlg nanofibers was achieved, the mat was formed rigidly and decreased after spider silk embedding, which may be attributed to the pore closure and hydrophobic polymers on the surface.

3.2. FE-SEM analyses of electrospun nanofiber mats

The morphology of electrospun nanofibers produced from 9 % w/v PVA - 1 % w/v NaAlg solution was seen in Fig. 1. A well distributed and uniform-continuous fiber formations were seen. The average fiber diameters were found to be 195 ± 38 nm for natural spider silk and 183 ± 35 nm for PVA/NaAlg/SS nanofiber mats, by measuring in FE-SEM's image post-processing program. Fig. 1 shows the surface morphological FE-SEM photos of PVA/NaAlg nanofiber mats, natural spider silk and PVA/NaAlg/SS nanofiber mats, respectively. As seen from the figure, PVA/NaAlg electrospun mat has fibers in transverse orientations without any nodes among the diameters.

3.3. XTT cell viability assay and cell adhesion studies

Cytotoxicity tests from XTT assays of cell viability and cytocompatibility in all groups were studied and the result is shown in Fig. 2. As a potential wound-dressing material for tissue/biomedical engineering, the wound dress should promote cell growth and physiological function and should be able to maintain normal states of cell differentiation. Fig. 2 demonstrated that all groups supported cell proliferation with cell viability values higher than 90 %. All groups show no signs of cytotoxicity. The highest activity was observed for PVA/NaAlg (122.4 ± 2.73) and PVA/NaAlg/SS (135.9 ± 4.82) nanofiber mats. However, there was no considerable difference in the cell activity between cotton gauze and Aquacel®-Ag groups and consequently proved beneficial for cell growth. Wound dressing surfaces play a vital role in cell adhesion and proliferation which can be analyzed using *in-vitro* cell adhesion studies. Fig. 3 shows the FE-SEM images of the mouse fibroblast cells (L929) seeded on the prepared groups. Compared to the control, Aquacel®-Ag and PVA/NaAlg group, PVA/NaAlg/SS groups showed improved cell attachment and proliferation. The reason is attributed to the presence of amino acid sequences in spider silk. The amino acid sequence act as cell receptors facilitating cell adhesion and growth [23]. The results proved that the developed nanofiber mats are highly biocompatible for tissue engineering applications.

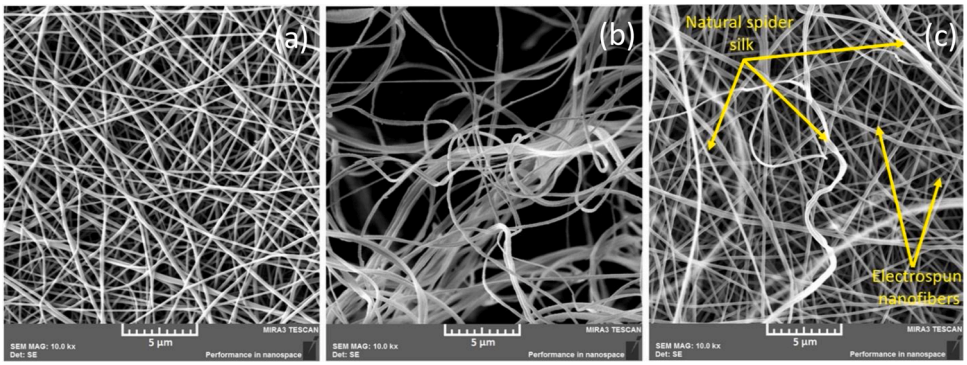

Fig. 1. FE-SEM photos of (a) electrospun PVA/NaAlg nanofiber mats, (b) natural spider silk and (c) electrospun PVA/NaAlg/SS nanofiber mats.

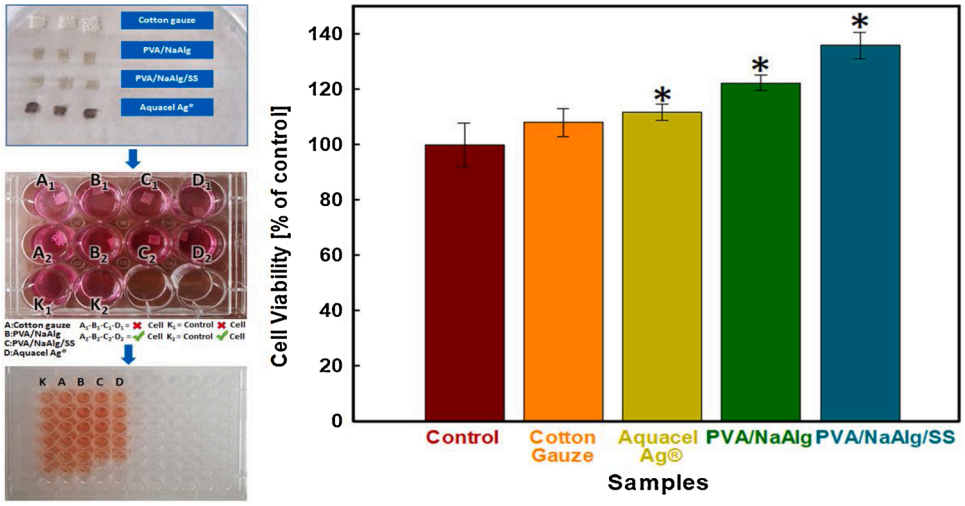

Fig. 2. Cell viability diagram by XTT assay (*p < 0.05).

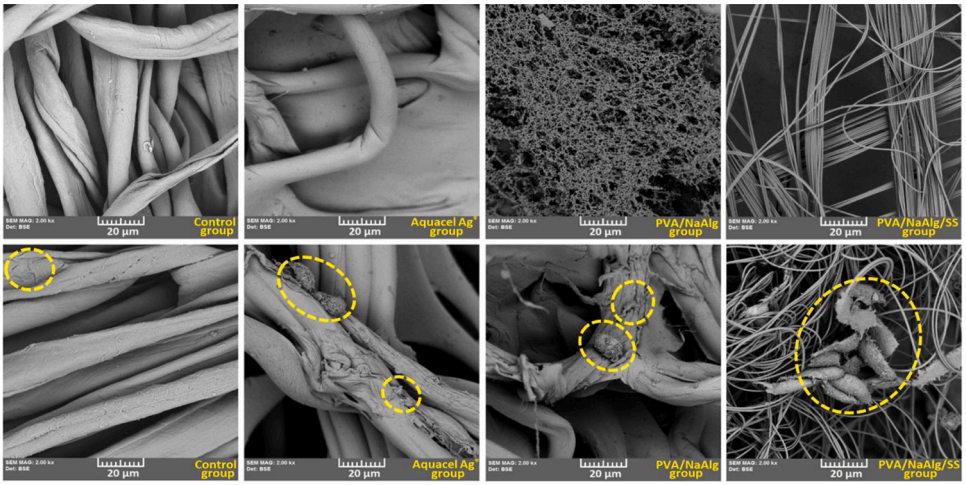

Fig. 3. FE-SEM micrographs representing cell attachment and growth after culturing for one day (above micrographs without cell and below micrographs with cell).

3.4. In-vivo wound healing studies using a healthy rabbit model

The representative wound images for the abrasion wound model on days 0, 4, 7, 12, 15, 18, and 21 are presented in Fig. 4. As seen from Fig. 4, the wound healing performance for all wound dressings was above 90 % from 12th day forward, and the wounds were almost entirely closed at the end of 21 days. At 4 days, wound closure in the treatment group (Aquacel®-Ag, PVA/NaAlg, PVA/NaAlg/SS) was not similar to the control group. As compared to untreated wounds, the commercial Aquacel®-Ag, PVA/NaAlg wound dressing product treated wounds and the novel PVA/NaAlg/SS treated wounds looked healthier and showed accelerated repair (Fig. 4). The wounds created in healthy rabbits with cotton gauze and Aquacel®-Ag healed at a slower rate as compared with PVA/NaAlg and PVA/NaAlg/SS wounds; the difference

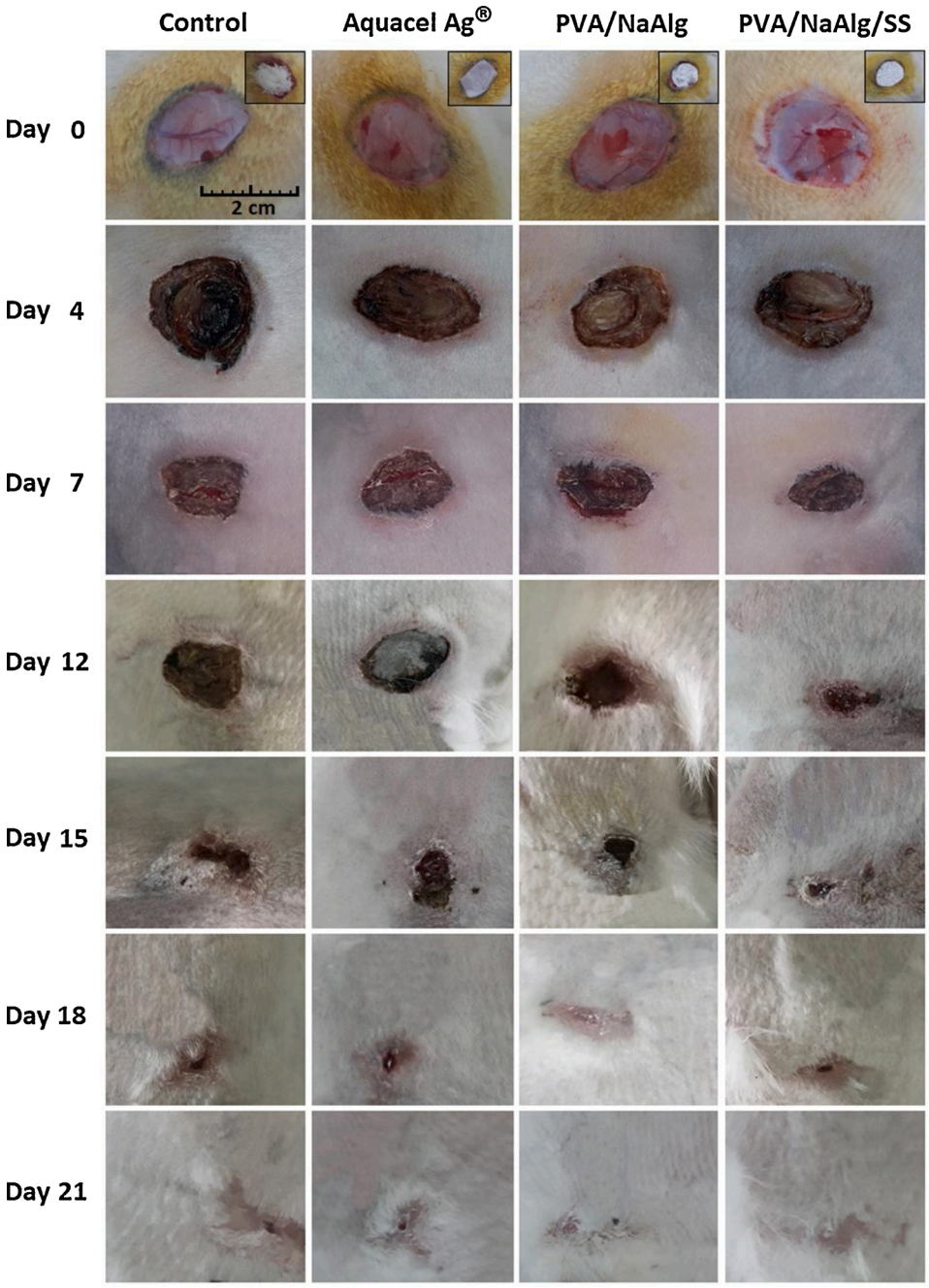

Fig. 4. Representative images of the wound model on post-treatment days.

was sharply visible on comparing the images of control wounds. Especially on the 7th and 12th day, the most rapid wound healing belonged to the wound area dressed with PVA/NaAlg/SS, following by PVA/NaAlg and Aquacel®-Ag nanofiber mats, respectively. The slowest wound healing was also eventuated on the wound area dressed in cotton gauze. Furthermore, swelling and inflammation were observed in the cotton gauze wounds, Aquacel®-Ag, and PVA/NaAlg groups on day 7, which continued on day 15.

3.5. Change in wound diameters depending on healing time

Fig. 5 shows the changes in the wound diameter in the rabbit groups at different healing times. The wounds remained stable in diameter for 16-h post-operation with a diameter of 20 ± 2 mm. The average diameters of the wounds linearly decreased until day 7, and by day 12 (15.7 ± 2.1 mm), the drastic decrease in the diameter of wounds occurred especially for PVA/NaAlg/SS nanofiber mats. As seen, it was obvious that the wound disappeared by day 15 for PVA/NaAlg/SS nanofiber mats. The PVA/NaAlg/SS nanofiber mats have not shown any significant hard scab during the healing period by both having the humidity in and out all the time and also by the antibacterial and anti-inflammatory cell effect of silk-fibroin. All group wounds were replenished every 2 days to keep the wound without a scab and to see the effect of materials. As indicated in Fig. 5, especially after day 12 the wound diameters of PVA/NaAlg and PVA/NaAlg/SS were much lower than other commercial Aquacel®-Ag and cotton gauze wound dresses. The measured values were 9.2 ± 0.5 mm, 6.03 ± 0.1 mm and 10.79 ± 0.5 mm, 12.06 ± 0.52 mm respectively. The control group has a healing period of irregular shape, and both the control and Aquacel®-Ag mats decrease the wound diameter linearly on day 15 while PVA/NaAlg/SS

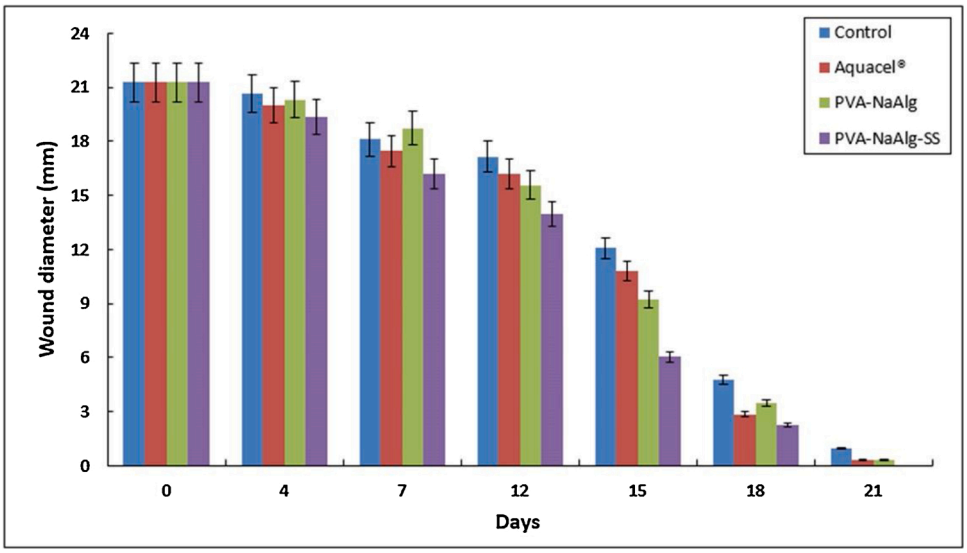

Fig. 5. Circular reduction of wounds' healing, extracted from the photos in Fig. 4 of photographic images of the extent of wound healing: graphical illustration of wound size changes on days 0, 4, 7, 12, 15, 18, and 21 under different treatment.

nanofiber mats left almost no wound to be healed even by day 18 than on day 21. The PVA/NaAlg/SS nanofiber mats showed a sudden decrease on day 7 healing the wound area down to 16 mm and followed by on day 15; the PVA/NaAlg/SS nanofiber mats decreased the area down to 5−6 mm while others are still around 18 mm and 9 mm, respectively for mentioned days. The diameter of the wound area covered by PVA/NaAlg/SS nanofiber mats was significantly lower than all other wound dressing and control.

Spider/silkworm silk biomaterial possesses huge potential in wound healing applications due to the inherent healing property of spidroin/fibroin. Despite having the intrinsic regenerative properties, combining silk fibroin biomaterials with other polymers or other bioactive factors could enhance the healing efficacy in various studies [24–26]. As shown in Figs. 4 and 5, the rabbit's wound size, treated with Aquacel®-Ag was observed much smaller than the control group on each time point, indicating the PVA/NaAlg/SS nanofiber matrices enhance the wound healing significantly. Moreover, spider silk addition improved the wound healing rate of the PVA/NaAlg nanofiber matrices compared

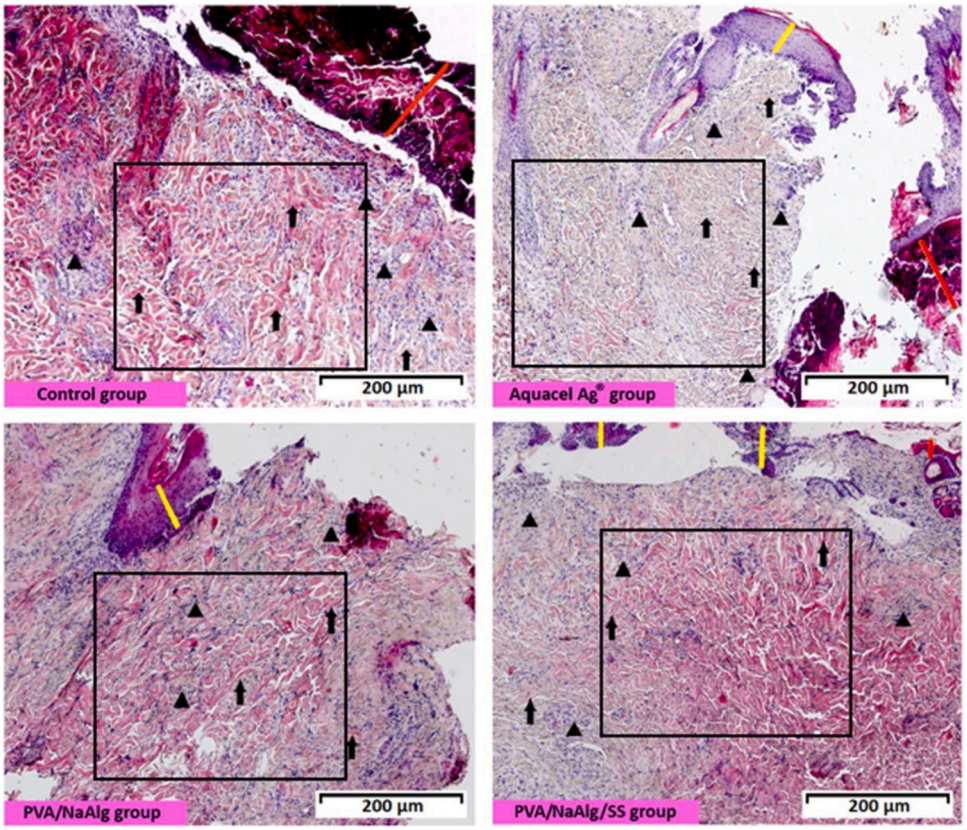

Fig. 6. Microscopic photographs of H&E-stained cross-sections of tissues obtained from regions covered by wound dressings on the 7th postoperative day (Magnification: ×10).

between the groups of PVA/NaAlg and Aquacel®-Ag (day 15). It was also observed that the wound treated with PVA/NaAlg/SS wound dressing showed a similar healing effect to that of the Aquacel®-Ag dressing (day 18).

3.6. Skin H&E Staining

In the histological evaluation state of *in-vivo* studies aiming to compare the wound healing performance of PVA/NaAlg and PVA/NaAlg/SS nanofiber mats with classical and commercial wound dressings, the effects of each dressing on wound healing were investigated. For this purpose, cross-sections of tissue samples obtained from wound areas covered by each dressing were microscopically examined on day 7 of wound formation. On the 7th postoperative day, the cross-section photographs of tissue samples obtained from regions covered by wound dressings are given in Fig. 6. On the 7th day of the control group's healing area, the presence of a thick scab tissue, in which epithelialization was not completed, is remarkable (red line). Inflammatory cells (black triangle) are densely located in the sub-epithelial healing region. At the same time, the collagen fibers are thin and irregular (black arrow). The first 7 days are critical in the wound healing period as very well known. The inflammation and proliferation phases are seen in these days. Histopathological evaluation of healing allows a rapid assessment of the tissue compatibility of the applied substance in material applications. [27]. We know that, the ideal procedure is to obtain 7th, 14th and 21st days for wound histopathology. However, in this case, to sacrifice fewer animals and to obtain a faster evaluation of produced data, this procedure was chosen as an indicator.

In the healing area of the Aquacel®-Ag group, it is noteworthy that epithelization was not completed (yellow line), the scab was present (red line), but epithelization started to occur on both sides of the wound area. Inflammatory cells (black triangle) are densely located in the sub-epithelial healing region. As shown in the image, collagen fibers are thicker but shorter and irregularly located than the control group (black arrow). It is noteworthy that epithelization in the PVA/NaAlg group's healing wound area is not complete (yellow line), and there is no scab. Inflammatory cells (black triangle) are densely located in the sub-epithelial healing region. The collagen fibers are thicker, but shorter and irregularly located than the control group (black arrow). For the healing wound area of the PVA/NaAlg/SS group, the epithelization is not complete (yellow line), the scab is present (red line). However, epithelization begins to occur in more areas than the other groups. Inflammatory cells (black triangle) are located in the sub-epithelial healing region. Collagen fibers are thicker and more regular than other groups (black arrow). The formation of granulation tissue (black rectangle) was faster in PVA/NaAlg/SS electrospun nanofiber mats treated wounds than in the other groups.

3.7. Morphological Structure and Texture Analysis of Collagens

One of the fibroblasts most important duties is the production of collagen. Collagen deposition is essential because it increases the wound strength; before it is laid down, the only thing holding the wound closed is the fibrin-fibronectin clot, which does not provide much resistance to traumatic injury. Also, cells involved in inflammation, angiogenesis, and connective tissue construction attach to, grow, and differentiate on the collagen matrix laid down by fibroblasts. Therefore, collagen plays a vital role in each phase of wound healing [28,29]. On day 7 of the wound healing site, the location, pattern, and thickness of the collagen fibrils were visualized by FE-SEM and showed in Fig. 7. The collagen

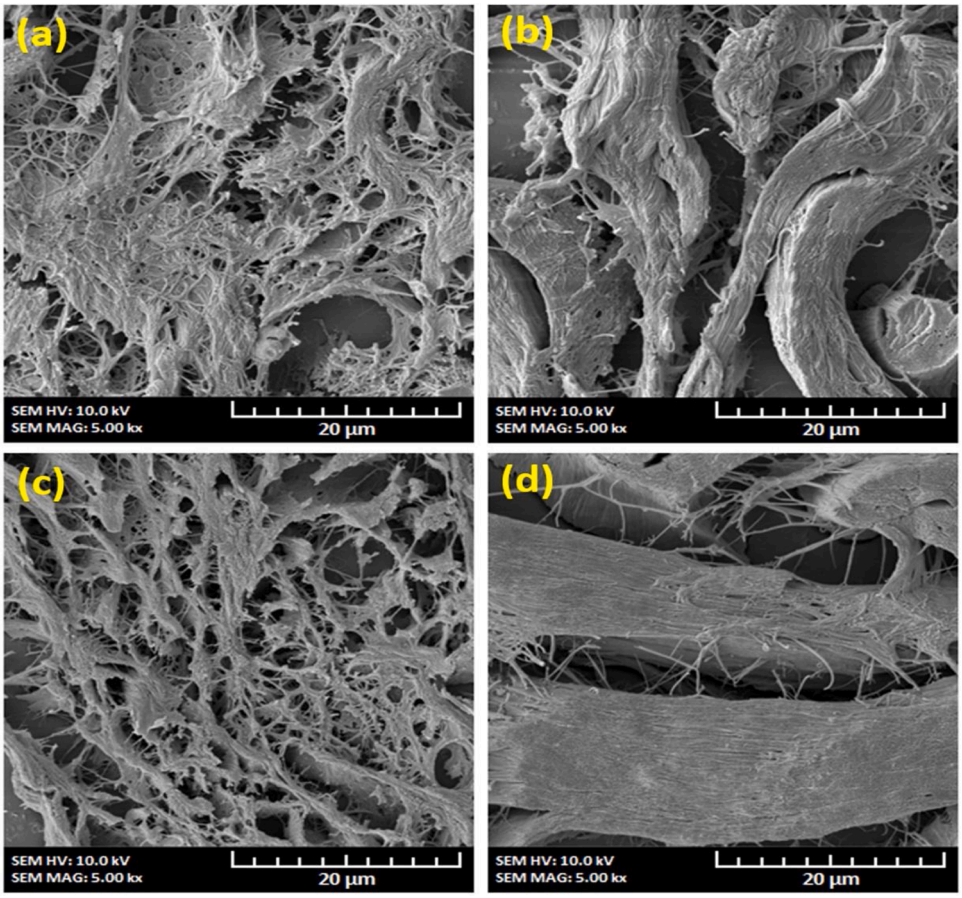

Fig. 7. FE-SEM images of tissues taken from under the wound healing site at seven days post-treatment (Magnification: ×5000). (a) Control group, (b) Aquacel®-Ag group, (c) PVA/NaAlg group, (d) PVA/NaAlg/SS group.

thickness values of obtained all groups are shown in Fig. 8. According to the FE-SEM examination, the collagen fibers were irregular and thin in control and the PVA/NaAlg group. In contrast, PVA/NaAlg/SS and Aquacel®-Ag group showed a thicker and more regular location. As seen in Fig. 7(a)–(c), the FE-SEM micrographs show a randomly disposed structure of thin fiber arrangements, with some more compact points in the matrix. In the control group, the fibers were entangled and clustered and more or less bundled above one another, leading to low dispersion and could not be effectively resulted.

For the Aquacel®-Ag, although there was relatively less thick collagen, the deposition amount was much more than that seen in the control and PVA/NaAlg group. The morphological structure and texture analysis of collagens were best visualized with the PVA/NaAlg/SS group. The thick fibers were too little crowded and neatly dispersed in the matrix.

The thickness of collagen in all groups was measured on the obtained FE-SEM photos. Results suggested that the collagen thickness (mm) in control, Aquacel®-Ag, PVA/NaAlg, and PVA/NaAlg/SS group was 2.03 ± 0.98 mm, 4.74 ± 1.73 mm, 2.06 ± 1.25 mm and 8.66 ± 2.61 mm, respectively.

With embedded spider silk into PVA/NaAlg, the measured collagen thickness in the reticular dermis increased significantly 7 days after treatment. It was visible in the matrix as compared with that of other groups (Fig. 7). The maximum thickness of collagen is present in PVA/NaAlg/SS group, whereas, in the control group, this thickness reaches a maximum reaching a value of 2.03 ± 0.98 mm. Furthermore, the collagen thickness in Aquacel®-Ag group was seen to be a similar trend with PVA/NaAlg/SS group. In contrast, the control and PVA/NaAlg groups did not show a well-organized deposition of thick collagen bundles.

Collagen is a natural component of the dermal matrix produced by fibroblasts and functions as a protective scaffolding for migrating epithelial cells in the regenerating skin. It attracts fibroblasts and keratinocytes to the wound and encourages debridement, angiogenesis, and re-epithelialization [30]. Studies have shown that VEGF is localized extensively in the healing area in the first 7 days, accelerates epithelialization, and the wound closes faster, activates fibroblasts, and starts to increase the amount in the wound area. VEGF has also been reported in studies that have been expressed from endothelial cells and accelerated the formation of new blood vessels [31–33].

As illustrated in Fig. 7 and graphed in Fig. 8, the membrane-like formation does not indicate the real formation of the collagen structure. This type of structure is also seen in Fig. 7(c) by the interconnecting fibrils between collagen fibrous. These are the baseline of the collagen that will be formed later on. Since the membrane-like structures are similar to each other for Fig. 8 (control group and PVA/NaAlg group)), the average thickness of the newly formed collagens is about 2 microns with a small positive deviation for PVA/NaAlg nanofiber mats.

Fig. 8 represents the Aquacel®-Ag and PVA/NaAlg/SS nanofiber mats to form new and thicker collagen fibers just under the wound healing areas. The Aquacel®-Ag is a unique newly developed commercial wound mat that has an oxygen permeability and antibacterial Ag^{+} containing mat to establish the wounds healing procedure by decreasing the inflammatory cell deposit around the wound while the antibacterial effect is also taking place. The PVA/NaAlg/SS nanofiber mat is another well-developed mat structure which is produced from spider made sterilized silk sericin-fibroin embedded on PVA/NaAlg nanofiber mats. The mats are UV sterilized, and sericin-fibroin is also an antibacterial material while maintaining good oxygen permeability as Aquacel®-Ag. Aquacel®-Ag forms collagen fibers with an average thickness of 4.7 ± 1.7 microns, while PVA/NaAlg/SS forms a unique and the thickest collagen fibers of 8.6 ± 2.6 microns. Besides, the collagen fibers are elongated and textured by very fine interconnecting fibrils between thick collagen fibers.

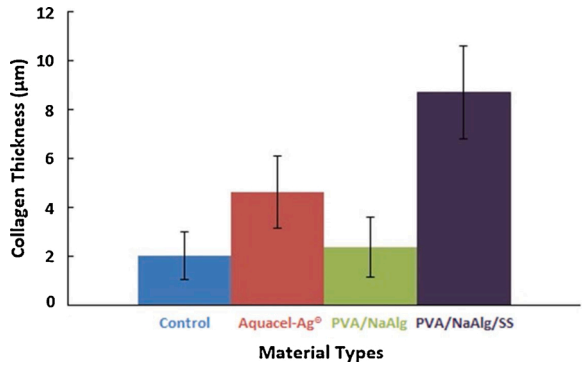

Fig. 8. The average collagen thickness of tissues.

3.8. Skin immunohistochemical staining (IHC)

Representative photomicrographs of immunohistochemical staining pattern showed in Fig. 9. In the VEGF immunohistochemically staining done in the control group, endothelial cells that they pre-exist in the improvement area and blood vessels that is nascent, in the cytoplasm's of fibroblasts which exist in peripheral and connective tissues VEGF immunolocalization has localization in apparent regions, and it is signed with red intensively. However, in the Aquacel®-Ag, group, it is indicated that improvement shows less localization than the group of PVA/NaAlg. In terms of immunolocalization, even though it shows more positivity in the disorganized area than the control group. In addition to this, the blood vessel that is nascent in the group of PVA/NaAlg is less than other groups, and VEGF localization occurs in the cell cytoplasms in the connective tissues. When PVA/NaAlg/SS groups are analyzed and compared, it is indicated that VEGF immunolocalization is high in both the cytoplasms of the cells that occur in the connective tissues and in the endothelial cell cytoplasm of the areas that have plenty of new blood vessels.

In our experimental study, VEGF localization was observed intensely in endothelial cells, fibroblast cytoplasm in the group we tested the spider silk. Increased VEGF immunolocalization in the spider silk group contributes to the formation of new blood vessels within the granulation tissue in the healing area, suggesting the fact that many cells migrate to the healing area with newly formed blood vessels, increasing the collagen production of fibroblasts, making this process faster than other groups. Our results indicated that PVA/NaAlg/SS wound dressings exhibited accelerated healing than other wound dressings, possibly because proteins such as silk glycoprotein, alanine, and glycine are bioactive and may promote adhesion, proliferation, migration, and skin regeneration [34]. It may be possible that, after treatment wound with spider silk embedded wound dressing, proliferation and re-modeling type processes are the dominant ones, since collagen synthesis increases, eventually leading to the improvement of the thickness of these collagen bundles, which is what we quantitatively proved [35]. These results indicate that natural spider silk can promote more collagen synthesis via activation of fibroblast formation, leading to the regeneration new tissues after injury.

4. Conclusions

In this study, novel electrospun nanofiber mats embedded with natural spider silk were successfully fabricated using the electrospinning method for wound dressing applications. The uniform and three-dimensional network of the nanofiber mats with well-designed and interconnected porosity among the nanofibers were proved by FE-SEM. The electrospun nanofiber mats revealed high porosity and water absorption coupled with adequate water vapor transmission. In addition, obtained nanofiber mats exhibited excellent cell proliferation, growth and cell adherence with embedding of natural spider silk into PVA/NaAlg nanofibers.

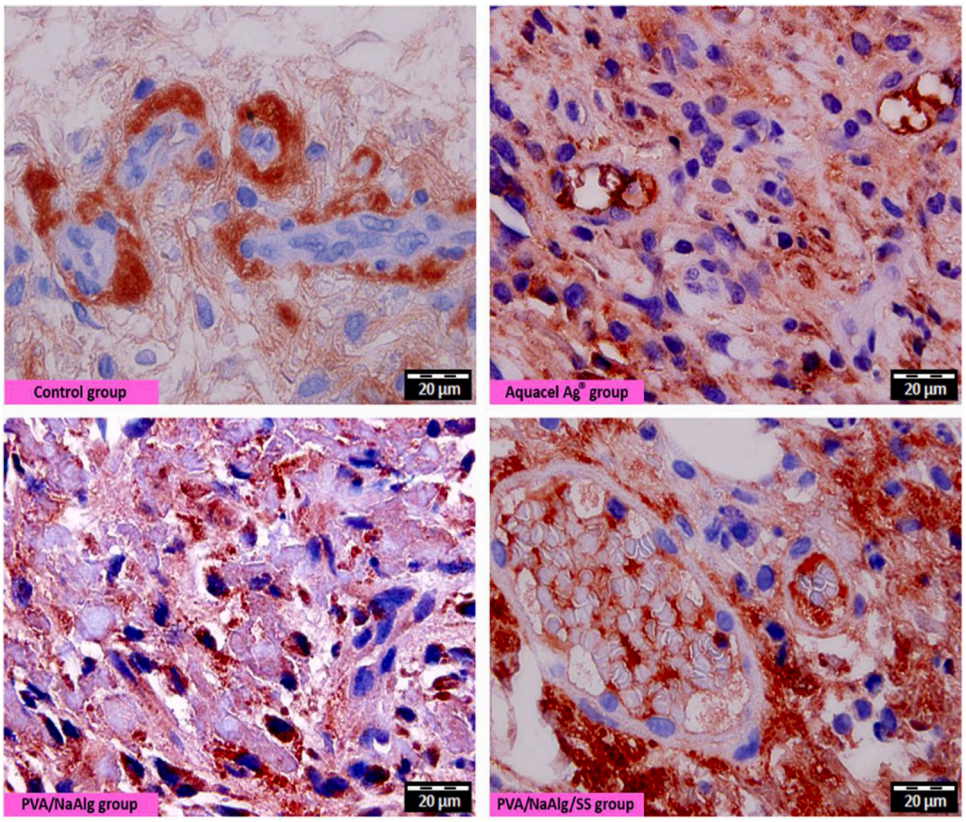

Fig. 9. Representative photomicrographs of the immunohistochemical staining pattern of the groups. (VEGF, Magnification: ×100). 7 days post-treatment below the wound area, the difference between VEGF immunolocalization leads to blood vessels' formation and is observed between them.

The recent reports were dealing with PVA or NaAlg separately, but our study aimed to combine synergistic effects of PVA/NaAlg/SS group. It was shown that a unique combination of faster wound healing without a scar and a thicker collagen tissue was formatted just under the skin. The PVA/NaAlg/SS group was seen as the best wound healing candidate material compared to Aquacel®-Ag group due to the thicker collagen formation as well as faster scar disappears, followed by a histological finding of inflammatory cell decreases around the wound even on the seventh day which makes the healing much faster. With VEGF immunohistochemical staining, the PVA/NaAlg/SS group was thought to have more VEGF immunolocalization than other groups, thereby increasing vascular structuring and healing in the healing area. The FE-SEM and histological microscopy images showed the faster scar closure and collagen formation up to a thickness of 9 µm in diameter, which is twice as thicker than the Aquacel®-Ag group and three times thicker than regular cotton gauze. The PVA/NaAlg/SS group can be said to be an excellent candidate material for rapid wound healing of skin scar. A quick future study is under construction to make these materials spread commercially after many other phase studies and the Ministry of Health's permission. It is planned to be studied on the concentration limits of SS on PVA/NaAlg mats.

Declaration of Competing Interest

The authors report no declarations of interest.

Acknowledgments

The authors would like to thank Sivas Cumhuriyet University Faculty of Medicine Research Center (CÜTFAM) for its technical support.

References

[1] M. Liu, X.P. Duan, Y.M. Li, D.P. Yang, Y.Z. Long, Electrospun nanofibers for wound healing, Mater. Sci. Eng. C 76 (2017) 1413–1423, https://doi.org/10.1016/j.msec.2017.03.034.
[2] E. Mele, Electrospinning of natural polymers for advanced wound care: towards responsive and adaptive dressings, J. Mater. Chem. B 28 (2016) 4801–4812, https://doi.org/10.1039/C6TB00804F.
[3] E. DeSimone, T.B. Aigner, M. Humenik, G. Lang, T. Scheibel, Aqueous electrospinning of recombinant spider silk proteins, Mater. Sci. Eng. C 106 (2020) 110–145, https://doi.org/10.1016/j.msec.2019.110145.
[4] S. Bhatia, Natural polymers vs synthetic polymer, in: S. Bhatia (Ed.), Natural Polymer Drug Delivery Systems: Nanoparticles, Plants, and Algae, Springer Cham., Switzerland, 2016, pp. 95–118.
[5] S. Sheik, S. Sheik, R. Nairy, G.K. Nagaraja, A. Prabhu, P.D. Rekha, K. Prashantha, Study on the morphological and biocompatible properties of chitosan grafted silk fibre reinforced PVA films for tissue engineering applications, Int. J. Biol. Macromol. 116 (2018) 45–53, https://doi.org/10.1016/j.ijbiomac.2018.05.019.
[6] M. Farokhi, F. Mottaghitalab, S. Samani, M.A. Shokrgozar, S.C. Kundu, R.L. Reis, Y. Fatahi, D.L. Kaplan, Silk fibroin/hydroxyapatite composites for bone tissue engineering, Biotechnol. Adv. 36 (2018) 68–91, https://doi.org/10.1016/j.biotechadv.2017.10.001.
[7] B. Kundu, R. Rajkhowa, C.S. Kundu, X. Wang, Silk fibroin biomaterials for tissue regenerations, Adv. Drug Deliv. Rev. 65 (2013) 457–470, https://doi.org/10.1016/j.addr.2012.09.043.
[8] F. Ruoqiu, L. Chenwen, Y. Caiping, X. Hong, S. Sanjun, L. Zhuoheng, W. Qing, L. Laichun, A novel electrospun membrane based on moxifloxacin hydrochloride/poly (vinyl alcohol)/sodium alginate for antibacterial wound dressings in practical application, Drug Deliv. 23 (2016) 828–839, https://doi.org/10.3109/10717544.2014.918676.
[9] P. Ni, H. Bi, G. Zhao, Y. Han, M.N. Wickramaratne, H. Dai, X. Wang, Electrospun preparation and biological properties in vitro of polyvinyl alcohol/sodium alginate/nano-hydroxyapatite composite fiber membrane, Colloid. Surf. B 173 (2019) 171–177, https://doi.org/10.1016/j.colsurfb.2018.09.074.
[10] A. Leal-Egana, T. Scheibel, Interactions of cells with silk surfaces, J. Mater. Chem. 22 (2012) 14330, https://doi.org/10.1039/c2jm31174g.
[11] Z. Setooni, M. Mohammadi, A. Hashemi, M. Hashemi, F. Mozafari, F. Simi, A. Bargahi, A. Daneshi, M.R. Hajiani-E-Asl, P. Farzadinia, Evaluation of wound dressing made from spider silk protein using in a rabbit model, Int. J. Low. Extrem. Wounds 17 (2) (2018) 71–77, https://doi.org/10.1177/15347346187828.

[12] M. Elices, G.V. Guinea, G.R. Plaza, C. Karatzas, C. Riekel, F. Agulló-Rueda, R. Daza, J. Pérez-Rigueiro, Bioinspired fibers follow the track of natural spider silk, Macromolecules 44 (5) (2011) 1166–1176, https://doi.org/10.1021/ma102291m.
[13] H. Adeli, M.T. Khorasani, M. Parvazinia, Wound dressing based on electrospun PVA/chitosan/starch nanofibrous mats: fabrication, antibacterial and cytocompatibility evaluation and in vitro healing assay, Int. J. Biol. Macromol. 122 (2019) 238–254, https://doi.org/10.1016/j.ijbiomac.2018.10.115.
[14] K. Kucharczyk, J.D. Rybka, M. Hilgendorff, M. Krupinski, M. Slachcinski, A. Mackiewicz, M. Giersig, H. Dams-Kozlowska, Composite spheres made of bioengineered spider silk and iron oxide nanoparticles for theranostics applications, PLoS One 14 (7) (2019) e0219790, https://doi.org/10.1371/journal.pone.0219790.
[15] H. Dams-Kozlowska, A. Majer, P. Tomasiewicz, J. Lozinska, D.L. Kaplan, A. Mackiewicz, Purification and cytotoxicity of tag-free bioengineered spider silk proteins, J. Biomed. Mater. Res. Part A 101 A (2013) 456–464, https://doi.org/10.1002/jbm.a.34353.
[16] X. Yang, L. Fan, L. Ma, Y. Wang, S. Lin, F. Yu, X. Pan, G. Luo, D. Zhang, H. Wang, Green electrospun Manuka honey/silk fibroin fibrous matrices as potential wound dressing, Mater. Des. 119 (2017) 76–84, https://doi.org/10.1016/j.matdes.2017.01.023.
[17] E. Danzer, U. Schwarz, S. Wehrli, A. Radu, N.S. Adzick, A.W. Flake, Retinoic acid induced myelomeningocele in fetal rats: characterization by histopathological analysis and magnetic resonance imaging, Exp. Neurol. 194 (2005) 467–475, https://doi.org/10.1016/j.expneurol.2005.03.011. 2005.
[18] Ü.S. Saraydın, Z.D. Şahin İnan, Myelin basic protein Ab-1 immunolocalization in rat nervous system, HealthMED 6 (2012) 392–394.
[19] Ü.S. Saraydin, D. Saraydin, Z.D. Şahin İnan, B. Özdenoğlu, The effects of monomers used in polymeric biomaterials on renal tissue, Int. J. Morphol. 35 (2017) 1203–1208, https://doi.org/10.4067/S0717-95022017000401203, 2017.
[20] Z.D. Şahin İnan, Ü.S. Saraydin, Immunohistochemical profile of CD markers in experimental neural tube defect, Biotechnic & Histochemistry 94 (2019) 617–627, https://doi.org/10.1080/10520295.2019.1622783.
[21] R.A. Walker, Quantification of immunohistochemistry issues concerning methods, utility and semiquantitative assessment I, Histopathology 49 (2006) 406–410, https://doi.org/10.1111/j.1365-2559.2006.02514.x.
[22] A. Anura, R.K. Das, M. Pal, R.R. Paul, A.K. Ray, J. Chatterjee, Correlated analysis of semi-quantitative immunohistochemical features of E-cadherin, VEGF and CD105 in assessing malignant potentiality of oral submucous fibrosis, Pathol. Res. Pract. 210 (2014) 1054–1063, https://doi.org/10.1016/j.prp.2014.06.009.
[23] L. Eisoldt, A. Smith, T. Scheibel, Decoding the secrets of spider silk, Mater. Today 14 (2011) 80–86, https://doi.org/10.1016/S1369-7021(11)70057-8.
[24] P. Kamalathevan, P.S. Ooi, Y.L. Loo, Silk-based biomaterials in cutaneous wound healing: a systematic review, Adv. Skin Wound Care 31 (2018) 565–573, https://doi.org/10.1097/01.ASW.0000546233.35130.a9.
[25] D. Chouhan, T.U. Lohe, P.K. Samudrala, B.B. Mandal, In situ forming injectable silk fibroin hydrogel promotes skin regeneration in full thickness burn wounds, Adv. Healthc. Mater 7 (2018) 1–15, https://doi.org/10.1002/adhm.201801092.
[26] E.S. Gil, B. Panilaitis, E. Bellas, D.L. Kaplan, Functionalized silk biomaterials for wound healing, Adv. Healthc. Mater. 2 (2013) 206–217, https://doi.org/10.1002/adhm.201200192.
[27] A.C.O. Gonzales, T.F. Costa, Z.A. Andrade, A.R.A.P. Medrado, Wound healing – a literature review, An Bras Dermatol. 91 (5) (2016) 614–620, https://doi.org/10.1590/abd1806-4841.20164741.
[28] D.G. Greenhalgh, The role of apoptosis in wound healing, Int. J. Biochem. Cell B. 30 (1998) 1019–1030, https://doi.org/10.1016/S1357-2725(98)00058-2.
[29] Z. Ruszczak, Effect of collagen matrices on dermal wound healing, Adv. Drug Deliv. Rev. 55 (2003) 1595–15611, https://doi.org/10.1016/j.addr.2003.08.003.
[30] N. Mariappan, Collagen dressing for thermal burns, S.J.A.M.S. 3 (2015) 58–61.
[31] A. Gopalakrishnan, M. Ram, S. Kumawat, S. Tandan, D. Kumar, Quercetin accelerated cutaneous wound healing in rats by increasing levels of VEGF and TGF-β1, Indian J. Exp. Biol. 54 (2016) 187–195.
[32] T.L. Cheng, P.K. Chen, W.K. Huang, C.H. Kuo, C.F. Cho, K.C. Wang, G.Y. Shi, H. L. Wu, C.H. Lai, Plasminogen/thrombomodulin signaling enhances VEGF expression to promote cutaneous wound healing, J. Mol. Med. 96 (2018) 1333–1344, https://doi.org/10.1007/s00109-018-1702-1.
[33] H. El-Gazaerly, D.M. Elbardisey, H.M. Eltokhy, D. Teaama, Effect of transforming growth factor Beta 1 on wound healing in induced diabetic rats, I.J.H.S. 7 (2013) 160–172, https://doi.org/10.12816/0006040.
[34] S. Hasatsri, A. Angspatt, P. Aramwit, Randomized clinical trial of the innovative bilayered wound dressing made of silk and gelatin: safety and efficacy tests using a split-thickness skin graft model, Evid.-Based Complement. Altern. Med. 5 (2015) 1–8, https://doi.org/10.1155/2015/206871.
[35] V. Marcos-Garcés, C. Bea Serrano, V. García Bustos, J. Benavent Seguí, A. Ferrández Izquierdo, A. Ruiz-Saur, Age-related dermal collagen changes during development, maturation and ageing – a morphometric and comparative study, J. Anat. 225 (2014) 98–108, https://doi.org/10.1111/joa.12186.